Appendix A. More Details on Track CHEM

The following provides additional details on Track CHEM of the competition.

Background on chemical reactions Parts of the following text are taken from Peters et al. (2022). A general reaction (for example Wilkinson, 2006) takes the form

$$m_1 R_1 + m_2 R_2 + \ldots + m_r R_r \to n_1 P_1 + n_2 P_2 + \ldots + n_p P_p,$$

where r is the number of reactants and p the number of products. Both R_i and P_j can be thought of as molecules and are often called species. The coefficients m_i and n_j are positive integers, called stoichiometries.

In mass-action kinetics (Waage and Guldberg, 1864), one usually considers the concentration $[X]$ of a species X, the square parentheses indicating that one refers to the concentration rather than to the integer amount of a given species. The concentration $[X]$ changes over time (but to simplify notation, we sometimes omit the notational dependence on t). The law of mass-action allows one to convert the above equations into a system of ODEs over the concentrations of species. Formally, it states: *The instantaneous rate of each reaction is proportional to the product of each of its reactants raised to the power of its stoichiometry.* To better understand how this can be applied to transform reaction equations into a system of ODEs, it may help to consider an example. The Lotka-Volterra predator-pray model (Lotka, 1909) can be expressed in terms of reactions of the form

$$A \xrightarrow{k_1} 2A \tag{8}$$

$$A + B \xrightarrow{k_2} 2B \tag{9}$$

$$B \xrightarrow{k_3} \emptyset, \tag{10}$$

where A and B describe abundance of prey and predators, respectively. In this model, the prey reproduce by themselves (8), but the predators require abundance of prey for reproduction, see (9). After some time, also the predators die (10). The coefficients k_1, k_2, and k_3 indicate the rates, with which the reactions happen (the larger the rates, the faster the reactions). Applying the law of mass-action yields the following system of ordinary differential equations (ODEs)

$$\tfrac{\mathrm{d}}{\mathrm{d}t}[A] = k_1[A] - k_2[A][B] \tag{11}$$

$$\tfrac{\mathrm{d}}{\mathrm{d}t}[B] = k_2[A][B] - k_3[B]. \tag{12}$$

Chemical reactions of the data-generating process The data-generating process is illustrated in Figure 1. The corresponding chemical reactions are given by

$$\begin{aligned}
&Z_1 + Z_2 \xrightarrow{k_1} Z_9 && Z_{10} \xrightarrow{k_5} Y && Z_{13} \xrightarrow{k_9} Z_1 + Z_2\\
&Z_3 + Z_4 \xrightarrow{k_2} Z_{10} && Z_{11} \xrightarrow{k_6} Y && Z_{14} \xrightarrow{k_{10}} Z_5 + Z_6.\\
&Z_5 + Z_6 \xrightarrow{k_3} Z_{11} && Z_9 + Y \xrightarrow{k_7} Z_{13} &&\\
&Z_7 + Z_8 \xrightarrow{k_4} Z_{12} && Z_{12} + Y \xrightarrow{k_8} Z_{14} &&
\end{aligned}$$

This system can be converted using the law of mass action resulting in the following ODE system.

$$\frac{\mathrm{d}}{\mathrm{dt}}[Z_1] = -k_1[Z_1][Z_2] + k_9[Z_{13}]$$
$$\frac{\mathrm{d}}{\mathrm{dt}}[Z_2] = -k_1[Z_1][Z_2] + k_9[Z_{13}]$$
$$\frac{\mathrm{d}}{\mathrm{dt}}[Z_3] = -k_2[Z_3][Z_4]$$
$$\frac{\mathrm{d}}{\mathrm{dt}}[Z_4] = -k_2[Z_3][Z_4]$$
$$\frac{\mathrm{d}}{\mathrm{dt}}[Z_5] = -k_3[Z_5][Z_6] + k_{10}[Z_{14}]$$
$$\frac{\mathrm{d}}{\mathrm{dt}}[Z_6] = -k_3[Z_5][Z_6] + k_{10}[Z_{14}]$$
$$\frac{\mathrm{d}}{\mathrm{dt}}[Z_7] = -k_4[Z_7][Z_8]$$
$$\frac{\mathrm{d}}{\mathrm{dt}}[Z_8] = -k_4[Z_7][Z_8]$$
$$\frac{\mathrm{d}}{\mathrm{dt}}[Z_9] = k_1[Z_1][Z_2] - k_7[Z_9][Y]$$
$$\frac{\mathrm{d}}{\mathrm{dt}}[Z_{10}] = k_2[Z_3][Z_4] - k_5[Z_{10}]$$
$$\frac{\mathrm{d}}{\mathrm{dt}}[Z_{11}] = k_3[Z_5][Z_6] - k_6[Z_{11}]$$
$$\frac{\mathrm{d}}{\mathrm{dt}}[Z_{12}] = k_4[Z_7][Z_8] - k_8[Z_{12}][Y]$$
$$\frac{\mathrm{d}}{\mathrm{dt}}[Z_{13}] = k_7[Z_9][Y] - k_9[Z_{13}]$$
$$\frac{\mathrm{d}}{\mathrm{dt}}[Z_{14}] = k_8[Z_{12}][Y] - k_{10}[Z_{14}]$$
$$\frac{\mathrm{d}}{\mathrm{dt}}[Y] = k_5[Z_{10}] + k_6[Z_{11}] - k_7[Z_9][Y] - k_8[Z_{12}][Y]$$

Evaluation For each of the systems, $i = 1, \dots, 12$, partipants were asked to provide control input for 50 initial values. Participants' control inputs were evaluated by running the data-generating process for each of the provided controls to compute the following loss for each system[5]

$$J_i := \frac{1}{50} \sum_{k=1}^{50} \left(\sqrt{\frac{1}{40} \int_{40}^{80} \left(Z_{15}^{i,k}(t) - y_*^{i,k} \right)^2 dt} + c \cdot \sqrt{\frac{||u^{i,k}||_2^2}{8}} \right), \tag{13}$$

where $c = \frac{1}{20}$ and $u^{i,k} \in \mathbb{R}^p$ is the control input provided by the participant corresponding to the kth initial condition in the ith system. The process $Y^{i,k}$ of course depends on the provided input, $u^{i,k}$, even though this is not made explicit in the notation.

A.1. CHEM results

The following table summarizes the results from Track CHEM. The keywords describing participants' solutions were chosen by the organizers based on participants' summaries of their solutions. *Oracle* corresponds to a solution using access to the true data generating process. *Oracle^e* corresponds to a solution generated with access to the true data generating process, but using only the expensive controls (see Section 3). *Zero* corresponds to a solution choosing $U \equiv 0$ for every system and initial condition.

Team name	Score	Place	Keywords
Oracle	0.0872		
Ajoo	0.0890	1st	Sparse estimation of graph Direct estimation of a function in $\mathcal{F}$
Oracle^e	0.1450		
TeamQ	0.3385	2nd	Neural network prediction of target
GuineaPig	0.3386	3rd	Neural network prediction of target
Zero	0.9686		

robot	dynamics (F)	specification (θ)	interface (A)
great-devious-beetle	Rotational2	$\theta^{\text{gr-be}}$	$A^{\text{de}} = \mathbf{1}_{2\times 2}$
great-vivacious-beetle		$\theta^{\text{gr-be}}$	$A^{\text{vi}} \in \mathbb{R}^{2\times 2}$
great-mauve-beetle		$\theta^{\text{gr-be}}$	$A^{\text{ma}} \in \mathbb{R}^{2\times 3}$
great-wine-beetle		$\theta^{\text{gr-be}}$	$A^{\text{wi}} \in \mathbb{R}^{2\times 4}$
rebel-devious-beetle		$\theta^{\text{re-be}}$	$A^{\text{de}} = \mathbf{1}_{2\times 2}$
rebel-vivacious-beetle		$\theta^{\text{re-be}}$	$A^{\text{vi}} \in \mathbb{R}^{2\times 2}$
rebel-mauve-beetle		$\theta^{\text{re-be}}$	$A^{\text{ma}} \in \mathbb{R}^{2\times 3}$
rebel-wine-beetle		$\theta^{\text{re-be}}$	$A^{\text{wi}} \in \mathbb{R}^{2\times 4}$
talented-ruddy-butterfly	Rotational3	$\theta^{\text{ta-bu}}$	$A^{\text{ru}} = \mathbf{1}_{3\times 3}$
talented-steel-butterfly		$\theta^{\text{ta-bu}}$	$A^{\text{st}} \in \mathbb{R}^{3\times 3}$
talented-zippy-butterfly		$\theta^{\text{ta-bu}}$	$A^{\text{zi}} \in \mathbb{R}^{3\times 4}$
talented-antique-butterfly		$\theta^{\text{ta-bu}}$	$A^{\text{an}} \in \mathbb{R}^{3\times 6}$
thoughtful-ruddy-butterfly		$\theta^{\text{th-bu}}$	$A^{\text{ru}} = \mathbf{1}_{3\times 3}$
thoughtful-steel-butterfly		$\theta^{\text{th-bu}}$	$A^{\text{st}} \in \mathbb{R}^{3\times 3}$
thoughtful-zippy-butterfly		$\theta^{\text{th-bu}}$	$A^{\text{zi}} \in \mathbb{R}^{3\times 4}$
thoughtful-antique-butterfly		$\theta^{\text{th-bu}}$	$A^{\text{an}} \in \mathbb{R}^{3\times 6}$
great-piquant-bumblebee	Prismatic	$\theta^{\text{gr-bu}}$	$A^{\text{pi}} = \mathbf{1}_{2\times 2}$
great-bipedal-bumblebee		$\theta^{\text{gr-bu}}$	$A^{\text{bi}} \in \mathbb{R}^{2\times 2}$
great-impartial-bumblebee		$\theta^{\text{gr-bu}}$	$A^{\text{im}} \in \mathbb{R}^{2\times 3}$
great-proficient-bumblebee		$\theta^{\text{gr-bu}}$	$A^{\text{pr}} \in \mathbb{R}^{2\times 4}$
lush-piquant-bumblebee		$\theta^{\text{lu-bu}}$	$A^{\text{pi}} = \mathbf{1}_{2\times 2}$
lush-bipedal-bumblebee		$\theta^{\text{lu-bu}}$	$A^{\text{bi}} \in \mathbb{R}^{2\times 2}$
lush-impartial-bumblebee		$\theta^{\text{lu-bu}}$	$A^{\text{im}} \in \mathbb{R}^{2\times 3}$
lush-proficient-bumblebee		$\theta^{\text{lu-bu}}$	$A^{\text{pr}} \in \mathbb{R}^{2\times 4}$

Table 1: Overview of the 24 robot systems used in Track ROBO. Here, θ^* refers to the robot specification (link lengths and masses, moments of inertia, friction coefficients, and locations of link center of masses) and $A^* \in \mathbb{R}^{q\times p}$ parametrizes the linear interface function; values are chosen at random, while the above table indicates which properties where shared across which robot systems. We refer to Appendix B.1 for details on the 2- and 3-link rotational robots' dynamics and to Appendix B.2 for details on the 2-link prismatic robots' dynamics.

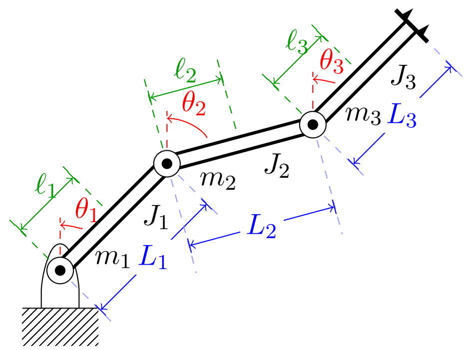

Figure 3: Diagram of a 3-link rotational robotic arm.

Appendix B. More Details on Track ROBO

Evaluation For each system (F^i, θ^i, A^i), $i \in \{1, \ldots, 24\}$ and repetition $k \in \{1, \ldots, 10\}$, running the system using the participants' controller and comparing the realized end-effector trajectory against a target process $z_*^{i,k} : [0, 2] \to \mathbb{R}^2$ the following loss is computed[5]

$$J_{i,k} := b_{i,k} \cdot \int_0^2 ||Z^{i,k}(t) - z_*^{i,k}(t)||_2^2 dt + c_{i,k} \cdot \int_0^2 U^{i,k}(t)^\top U^{i,k}(t) dt, \tag{14}$$

where $b_{i,k}$ and $c_{i,k}$ are scaling constants which are selected such that $J_{i,k} = 100$ when no controls are applied and $J_{i,k} = 1$ if an oracle LQR-controller is used, that is, an LQR-controller using the true robot dynamics and interface function. If $J_{i,k}$ is smaller than 1, it is improving on the oracle LQR-controller; if it is larger than 100 the performance is worse than when doing nothing. We clip all scores at 100 before averaging them. The scaling is meant to ensure that losses are comparable across each repetition.

For the (preliminary) leaderboard, which was updated during the competition, only 12 systems were evaluated, and the mean loss across those systems (and all corresponding repetitions) was shown on the leaderboard. For the final ranking, the average loss across the 12 held-out systems (and all corresponding repetitions) was used.

B.1. Rotational robots

We consider two types of rotational robotic manipulators: open chain planar manipulators with three (cf. Figure 3) and two revolute joints. Joints can be controlled by applying a voltage signal to a DC motor located in the joint, which creates a torque.

We begin with discussing the 3-link manipulator and then show the simplified version for the 2-link variant. Let $Z(t) = [\theta_1(t), \theta_2(t), \theta_3(t), \omega_1(t), \omega_2(t), \omega_3(t)]^\mathrm{T} \in \mathbb{R}^6$ be the state of the robotic arm, consisting of joint angles $(\theta_1, \theta_2, \theta_3)$ and corresponding angular velocities $(\omega_1, \omega_2, \omega_3)$. Let $U(t) = [\tau_1(t), \tau_2(t), \tau_3(t)]^\mathrm{T} \in \mathbb{R}^3$ be the input joint torques (τ_1, τ_2, τ_3).

The robotic arm is characterized by the following properties for the links, $i \in \{1, .., 3\}$:

- m_i is the link mass,
- J_i is the link rotational moment of inertia,

5. The integrals are approximated numerically.

- L_i is the link length,
- ℓ_i is the location of the link center of mass, and
- c_i is the joint rotational friction coefficient.

The second-order dynamic system of the robotic arm is expressed through the following set of first-order equations (Jian and Zushu, 2003):

$$\begin{aligned}
\tfrac{\mathrm{d}}{\mathrm{dt}}[\theta_1] &= \omega_1 \\
\tfrac{\mathrm{d}}{\mathrm{dt}}[\theta_2] &= \omega_2 \\
\tfrac{\mathrm{d}}{\mathrm{dt}}[\theta_3] &= \omega_3 \\
\tfrac{\mathrm{d}}{\mathrm{dt}}[\omega_1] &= \alpha_1 \\
\tfrac{\mathrm{d}}{\mathrm{dt}}[\omega_2] &= \alpha_2 \\
\tfrac{\mathrm{d}}{\mathrm{dt}}[\omega_3] &= \alpha_3
\end{aligned}$$

The joint acceleration terms $\alpha = [\alpha_1, \alpha_2, \alpha_3]^{\mathrm{T}}$ are determined via:

$$\alpha = M^{-1} (\tau - C\omega - N) \tag{15}$$

where the inertia matrix M, Coriolis matrix C, and external force vector N are:

$$M = \begin{bmatrix} M_{11} & M_{12}\cos(\theta_2 - \theta_1) & M_{13}\cos(\theta_3 - \theta_1) \\ M_{12}\cos(\theta_2 - \theta_1) & M_{22} & M_{23}\cos(\theta_3 - \theta_2) \\ M_{13}\cos(\theta_3 - \theta_1) & M_{23}\cos(\theta_3 - \theta_2) & M_{33} \end{bmatrix},$$

$$C = \begin{bmatrix} 0 & C_{12}\sin(\theta_2 - \theta_1)\omega_2 & C_{13}\sin(\theta_3 - \theta_1)\omega_3 \\ C_{21}\sin(\theta_2 - \theta_1)\omega_1 & 0 & C_{23}\sin(\theta_3 - \theta_2)\omega_3 \\ -C_{13}\sin(\theta_3 - \theta_1)\omega_1 & C_{32}\sin(\theta_3 - \theta_2)\omega_2 & 0 \end{bmatrix}, \text{ and}$$

$$N = \begin{bmatrix} N_1\sin(\theta_1) + c_1\omega_1 \\ N_2\sin(\theta_2) + c_2\omega_2 \\ N_3\sin(\theta_3) + c_3\omega_3 \end{bmatrix}$$

with coefficients

$$\begin{aligned}
M_{11} &= m_1\ell_1^2 + J_1 + (m_2 + m_3)L_1^2 \\
M_{12} &= (m_2\ell_2 + m_3L_2)L_1 \\
M_{13} &= m_3\ell_3L_1 \\
M_{22} &= m_2\ell_2^2 + J_2 + m_3L_2^2 \\
M_{23} &= m_3\ell_3L_2 \\
M_{33} &= m_3\ell_3^2 + J_3 \\
C_{12} &= -(m_2\ell_2 + m_3L_2)L_1 \\
C_{13} &= -m_3\ell_3L_1 \\
C_{21} &= (m_2\ell_2 + m_3L_2)L_1 \\
C_{23} &= -m_3\ell_3L_2 \\
C_{32} &= m_3\ell_3L_2 \\
N_1 &= -(m_1\ell_1 + (m_2 + m_3)L_1)g \\
N_2 &= -(m_2\ell_2 + m_3L_2)g \\
N_3 &= -m_3\ell_3g
\end{aligned}$$

and g is gravitational acceleration.

For the 2-link robot, we omit all terms that correspond to the third joint. That is, the acceleration $\alpha = [\alpha_1, \alpha_2]^{\mathrm{T}}$ is still given by (15), but we now need to adapt M, C, and N. When only considering two joints, we have

$$\begin{aligned}
M &= \begin{bmatrix} M_{11} & M_{12}\cos(\theta_2 - \theta_1) \\ M_{12}\cos(\theta_2 - \theta_1) & M_{22} \end{bmatrix} \\
C &= \begin{bmatrix} 0 & C_{12}\sin(\theta_2 - \theta_1)\omega_2 \\ C_{21}\sin(\theta_2 - \theta_1)\omega_1 & 0 \end{bmatrix} \\
N &= \begin{bmatrix} N_1\sin(\theta_1) + c_1\omega_1 \\ N_2\sin(\theta_2) + c_2\omega_2 \end{bmatrix}
\end{aligned}$$

with coefficients

$$\begin{aligned}
M_{11} &= m_1\ell_1^2 + J_1 + m_2L_1^2 \\
M_{12} &= m_2\ell_2L_1 \\
M_{22} &= m_2\ell_2^2 + J_2 \\
C_{12} &= -m_2\ell_2^2L_1 \\
C_{21} &= m2\ell_2L_1 \\
N_1 &= -(m_1\ell_1 + m_2L_1)g \\
N_2 &= -m_2\ell_2g.
\end{aligned}$$

Remark 1 *Note that in the open source code, we define the joint angles of the 2-link manipulator with respect to each other instead of with respect to the vertical axis (Murray et al. (2017)). Hence, the equations slightly differ from the ones presented above. However, the dynamics are the same as described herein.*

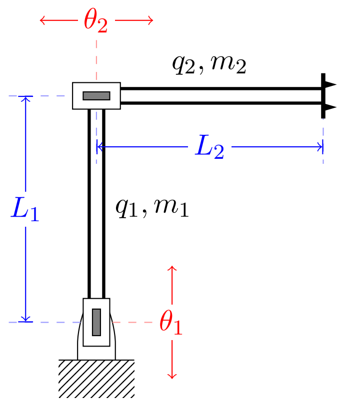

Figure 4: Diagram of the 2-link prismatic robot arm.

B.2. Prismatic robot

Besides the two versions of rotational robots, we also consider a 2-link prismatic robot arm (Figure 4). This idealized prismatic robot is actuated by prismatic joints that change the link lengths, such that $L_i = q_i + \theta_i$, where q_i represents the link length at zero joint input. Although the link length changes, we assume the link mass m_i remains constant.

Due to the lateral instead of rotational movements, the dynamics of this robot are considerably simpler. The joint acceleration terms $\alpha = [\alpha_1, \alpha_2]^{\mathrm{T}}$ are given by

$$\alpha = M^{-1} (\tau - N) . \tag{16}$$

The equation is similar to (15), but without the Coriolis term since there are only lateral movements. Mass matrix and external force vector are $M = \begin{bmatrix} m_1 + m_2 & 0 \\ 0 & m_2 \end{bmatrix}$ and $N = \begin{bmatrix} g(m_1 + m_2) \\ 0 \end{bmatrix}$, respectively.

B.3. ROBO results

The results from Track ROBO are summarized below. The keywords were chosen by the organizers based on the participants' descriptions of their approaches. The score function is standardized such that a value of 1 corresponds to the performance of an oracle LQR-controller using the true system (optimizing only the trajectory, not the cost). A score of 100 corresponds to the zero solution, $U \equiv 0$.

Team name	Score	Place	Keywords
Ajoo	0.918	1st	Estimation of robot dynamics
TeamQ	16.121	2nd	Neural network prediction
jmunozb	29.539	3rd	Linear system approximation Regression with polynomial features